



## Research article

## Effect of ionic surfactants on the settling behavior of silt

Zhuo Huang<sup>a,\*</sup>, Yuan Xiang<sup>b</sup>, Yue-Xiao Liu<sup>c</sup>, Guang-Fang Li<sup>d</sup>, Hui-Qun Cao<sup>c</sup><sup>a</sup> Ecological Restoration Technology Center, Changjiang River Scientific Research Institute, No. 23 Huangpu Avenue, Wuhan, People's Republic of China<sup>b</sup> Environment Technology Branch, Wuhan Changjiang Kechuang Technology Development Co., Ltd., No. 289 Huangpu Avenue, Wuhan, People's Republic of China<sup>c</sup> Department of Water Environment Research, Changjiang River Scientific Research Institute, No. 23 Huangpu Avenue, Wuhan, People's Republic of China<sup>d</sup> School of Chemistry and Chemical Engineering, Huazhong University of Science and Technology, No. 1037 Luoyu Road, Wuhan, People's Republic of China

## ARTICLE INFO

## Keywords:

Cetyltrimethylammonium bromide  
Linear alkylbenzene sulfonate  
Flocculation  
Settling velocity  
Zeta potential  
Surface tension

## ABSTRACT

Ionic surfactants are easily adsorbed by silt and clay particles, thus affecting the flocculation characteristics and settling behavior. The settling velocity, typical size, Zeta potential and surface tension of silt flocs were measured in the presence of two different kinds of ionic surfactants. The results indicated that the cetyltrimethylammonium bromide (CTAB, a typical cationic surfactant) can dramatically accelerate the settling of silt particles, while the linear alkylbenzene sulfonate (LAS, a typical anionic surfactant) slightly retarded silt sedimentation to some extent. In still water, the representative settling velocity dramatically increased from  $0.36 \text{ cm s}^{-1}$  to  $0.43 \text{ cm s}^{-1}$  with the increase of CTAB concentration, which increased by more than 20%. Oppositely, the sedimentation rate decreased from  $0.36 \text{ cm s}^{-1}$  to  $0.33 \text{ cm s}^{-1}$  with the increase of LAS concentration. In flowing water, as the flow rate increased from 0 to  $20 \text{ cm s}^{-1}$  and the ionic surfactant concentration increased from 0 to  $10 \text{ mg L}^{-1}$ , the sedimentation rate decreased to 57% and 89% in the presence of CTAB and LAS respectively, which was due to an enhanced dispersion of silt particles and a breaking of flocs. The SEM image test shows that the floc particle size increased 1.5 times of the primary particle size under the high CTAB concentration. The flocculation induced by ionic surfactants greatly influences the sediment size as well as the law of settling velocity. The intrinsic influence mechanism was also discussed based on the variations of silt particle properties. This systematic study can be used for further development of flocculation models and particle size distribution of fine-grained soil.

## 1. Introduction

Ionic surfactants have been broadly applied in detergent, fiber softener and disinfectant for daily life and industrial use, as well as pesticide products [1], along with domestic sewage and industrial wastewater, they were discharged into rivers and lakes. Based on DLVO theory, the ionic surfactant can be rapidly adsorbed by sediments with particle size less than 0.100 mm (known as fine-silt and clay) [2] due to the structure of the diffused double electric layer and negative charge on the surface of sediment. The forces between sediment particles then change, resulting in flocculation. Accordingly, sediment dynamics such as sediment incipient motion,

\* Corresponding author.

E-mail address: [huangzhuo@mail.crsri.cn](mailto:huangzhuo@mail.crsri.cn) (Z. Huang).

<https://doi.org/10.1016/j.heliyon.2023.e15669>

Received 3 January 2023; Received in revised form 18 April 2023; Accepted 18 April 2023

Available online 21 April 2023

2405-8440/© 2023 The Authors. Published by Elsevier Ltd. This is an open access article under the CC BY-NC-ND license (<http://creativecommons.org/licenses/by-nc-nd/4.0/>).

suspension, and re-suspension, especially the sedimentation, will be significantly affected and changed. Along the sediment-laden rivers, especially estuaries, fine-silt and clay usually exist as suspended sediment, providing excellent substratum for the attachment of ionic surfactants and the formation of flocs. Knowledge of sediment settling processes in the presence of ionic surfactants is necessary to better understand, simulate and predict the sediment transport dynamics in natural water. Therefore, it is of great significance to solve such problems as river estuary regulation and maintenance, and water ecological environment protection [3].

The effect of flocculation on flocs characteristics and sediment dynamics is a complex systematic problem, and many scholars have done a lot of research in the past decades. It is known that there are many factors affecting the flocculation process and flocs features, mainly including the properties of primary sediment particles, turbulent shear, suspended sediment concentration, salinity, inorganic ions, organic matter, temperature, pH and so on.

The size of flocs in suspension has been found to be several times larger than the primary size of the sediment, which is mainly controlled by turbulence and organic matter content more than any other parameters [4–6]. With the increasing turbulent shear rate, the frequency of collision between sediment particles increases, thus promoting the formation of flocs. But when the turbulent shear rate increases to a critical value, resulting in the breakup of large and loose flocs [7]. Unlike turbulence, organic matter and its biopolymers in the water environment have been found to enhance both flocculation and stabilization [8]. With the increase of organic matter content, the particle size of flocs increases first and then decreases [9,10]. Furthermore, the effect of sediment suspension concentration on the flocculation process has been shown to be similar to that of turbulence, but not to the same extent [11]. It has also been found that the development of flocculation was promoted by the increasing temperature and vertical gradient of salinity [12], reaching its strongest when pH is between 8.5 and 12 [13].

Except for the size of sediment flocs, the settling rate of flocs has been taken as another fundamental parameter by sediment researchers. The accurate determination is regarded as a top priority in improving numerical modelling and conceptual understanding of sediment dynamics. The sedimentation process has been found to be affected by many factors. Among them, suspended sediment concentration (SSC), salinity and temperature all affect settling velocity, but to different extents [14]. The peak of settling velocity occurs within an optimum SSC, salinity and temperature range because of the non-monotonic properties [15]. Moreover, the settling rate of sediment particles decreases with increasing pH [16]. It has also been found that the settling velocity increases with increasing cation concentration. But when the cation concentration exceeds the critical concentration, little change occurs in spite of the sharp increase of cations concentration.

Unlike inorganic ions and nonionic organic substances, ionic surfactant molecules have long carbon chains and hydrophilic oleophilic amphiphilic properties [1]. Once the silt particles adsorbed ionic surfactants, the surface characteristics such as surface tension at the solid-liquid interface, immediately change, resulting in sediment transport behavior changes. Therefore, it is of great significance to investigate the effect of exogenous ionic surfactants on the settling behavior of silt particles in water. However, there is no relevant research available about this. In this study, cetyltrimethylammonium bromide (CTAB) and linear alkylbenzene sulfonate (LAS) were selected as the typical cationic and anionic surfactants respectively. The effect of ionic surfactant on silt settlement was investigated by testing the settling velocity, measuring the values of Zeta potential and surface tension as well as scanning electron microscope images (SEM). Finally, the intrinsic influence mechanism of the ionic surfactant was discussed.

## 2. Materials and methods

### 2.1. Study design

The sedimentation experiment in flowing water was conducted in a specially designed annular flow-simulation device in December 2019, as shown in Fig. 1. The device is composed of plexiglass annular tank, water pump, velocity control, measurement unit, pH meter, water gauge, sampling hole, valves and so on, which can control the flow rate, ensure the uniformity of flow and silt mixing, and facilitate subsequent sampling.

Materials and instruments used in the hydrostatic sedimentation test: scanning electron microscope (SEM, Regulus8100, Hitachi), fully automatic surface tensiometer (USA KINO Industry Co., Ltd.), laser particle size analyzer (Mastersizer 3000, Malvern Instrument

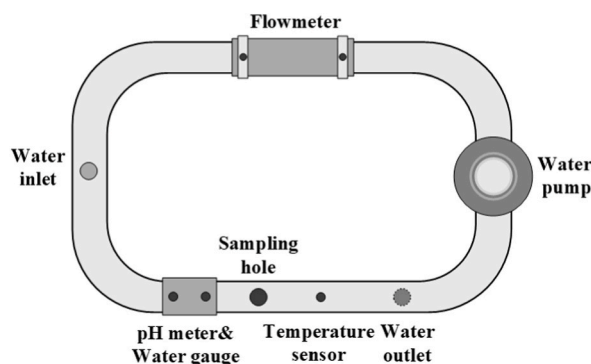


Fig. 1. Schematic diagram of annular flow-simulating experiment device.

Co., Ltd.), Zeta potentiometer (Malvern Instrument Co., Ltd.), specific surface and aperture meter (JW-BK122F, Beijing Jingwei Gaobo Technology Co., Ltd.), air bath thermostatic oscillator (BSD-YX2400, Shanghai Boxun Medical Bio-instrument Ltd.), water purification machine (MERCK MILLIPORE Aquelix 5), 50 mL pycnometer (Sichuan Yak Glass Instrument Co., Ltd.), 0.45  $\mu\text{m}$  microporous membrane (Shanghai Xinya Purification Device Factory), 1000  $\text{mg L}^{-1}$  CTAB solution, 1000  $\text{mg L}^{-1}$  LAS solution.

## 2.2. Sampling

The silt samples were taken from the middle reaches (Wuhan) of Yangtze River by using the sediment sampler in mid-July 2019 (rainy season). Three sampling points were set along the left and right banks in the reach of the river. The sampling depth was 0–30 cm below the bed surface, and 1 kg bed material was collected at each sampling point. There was a pretreatment procedure conducted in 2 L baker to wipe off the absorbed other metal cations and organic matter by means of hydrochloric acid and concentrated nitric acid with 20%  $\text{H}_2\text{O}_2$ , respectively. After that, the silt samples were placed into an oven at 105  $^\circ\text{C}$  for 8 h until silt water content was below 1%. Only then were they transferred to a desiccator. The grain-size distribution of the primary silt samples is in the range of 3–110  $\mu\text{m}$ . After screening, the particle size group ( $>62 \mu\text{m}$ ) was taken as the test samples. The particle specific surface area and total pore volume were obtained by BET (Brunauer-Emmett-Teller) method and BJH (Barret-Joyner-Halenda) method respectively. The physical properties of primary silt samples were listed in Table 1.

## 2.3. Experimentation

### 2.3.1. Silt settling test under the influence of ionic surfactants

The settling test of silt in still water was completed in a 1 L measuring cylinder and the initial silt concentration was set to 3  $\text{g L}^{-1}$ . The sampling time was set to 15 s, 30 s, 1 min, 5 min and every 5 min until 150 min. The initial surfactant concentration was set to 0, 5, 10, 15 and 20  $\text{mg L}^{-1}$ . Corresponding concentration of the ionic surfactant solution was prepared in the measuring cylinder at  $18 \pm 0.5 \text{ }^\circ\text{C}$ . In order to avoid the influence of trace minerals and impurities in water on the soil-related test, the purified water used in this experiment was all deionized water (DI water), which can remove all anions and cations in the water by double treatment of reverse osmosis membrane and mixed bed resin. Firstly, the silt sample of 3 g was dispersed with an appropriate amount of DI water by the ultrasonic wave for 30 min. Secondly, the suspended silt solution was poured into the measuring cylinder and DI water was added to the 1 L mark. In order to make silt evenly distributed in the measuring cylinder, the mixture was stirred vigorously for 20 s with a three-layer spiral stirring rod, and then stirred up and down for 1 min more than 30 times. After the stirring stopped, samples were taken at regular intervals, 20 cm below the center of the measuring cylinder with a 10 mL pipette, and transferred to the sand cup as soon as possible. Finally, the silt sample in the sand cup was filtered, the real-time silt content was measured by the dry weighing method and repeated three times for each experimental condition.

The settling test of silt in flowing water was carried out in the annular flow-simulating experiment device. The water velocity was controlled by flowmeter and the temperature was maintained at  $18 \pm 0.5 \text{ }^\circ\text{C}$ . The initial ionic surfactant concentration was set to 0, 1, 3, 5, and 10  $\text{mg L}^{-1}$ , the flow velocity was 20, 10 and 0  $\text{cm s}^{-1}$ , and the silt content at each velocity was measured at 5, 10, 15, 17, 20, 30, and 60 min, respectively. First, the water and silt were well mixed at a high spin speed, then the silt suspension samples at a depth of 2 cm below liquid surface were taken from the sampling hole to measure the real-time silt content when the equilibrium concentration was reached.

### 2.3.2. SEM observation

The silt samples adsorbed and balanced under different concentrations of surfactants were placed in a glass evaporating dish and lyophilized for 48 h in a vacuum freeze dryer. A portion of the silt sample was scraped off and prepared by vacuum spray with gold. Then SEM image was obtained with a grayscale of 256 and gray value range scale of 0–255.

### 2.3.3. The measurement of zeta potential and surface tension

The silt suspension affected by the ionic surfactant was taken from 10 cm below the liquid surface. The average value was measured three times by Zeta Potentiometer to record the Zeta potential of the solution under the influence of variable concentrations of ionic surfactant. The Zeta potential has been estimated by electrophoretic measurements (Malvern Zetasizer 1000HS/3000HS) using the Smoluchowski equation. Besides, the surface tension of the mixture of silt and ionic surfactant solution was measured by the platinum ring method.

## 2.4. Data processing

According to the normal distribution of the measured data, data samples with standard deviation more than 2 times were excluded,

**Table 1**  
Physical properties of primary silt samples.

particle size range ( $10^{-6}$ ) (m)	specific surface area ( $10^3$ ) ( $\text{m}^2 \text{kg}^{-1}$ )	total pore volume ( $10^{-3}$ ) ( $\text{m}^3 \text{kg}^{-1}$ )	bulk density ( $10^{-3}$ ) ( $\text{kg m}^{-3}$ )	pH value of water-silt mixture
62–110	5.704	0.035	2.739	7.25–8.27

and the average value of the remaining sample data was adopted for calculation.

### 3. Results

#### 3.1. Effect of ionic surfactant concentration on silt settling

The time-dependent suspended silt concentration at 20 cm below the free surface was investigated in the presence of different CTAB concentrations in still water, as shown in Fig. 2(a). For all cases, a sharp decrease of suspended concentration occurred in the first 15 min and then no substantial decrease was observed. The settling velocity of silt increased with the increase of CTAB concentration. Taking the derivative of these curves, the catastrophe points were all located at 35 min. Therefore, it can be suggested that the settling velocity is changed by the particle flocculation in the presence of CTAB. At the beginning of the settlement test, the particle content of the whole settling column was relatively uniform. Soon after, some primary silt particles began to collide and aggregate into flocs under the action of CTAB. It can also be predicted that these flocs have larger size and faster settling velocity than primary particles.

Differentiating from CTAB, LAS had less influence on the change of suspended silt concentration, as shown in Fig. 2(b). As the increase of LAS concentration, there was no significant change in the silt settling velocity. It can be easily found that the effect of CTAB on silt settling velocity is much greater than that of LAS under the same conditions of ionic surfactant concentration and initial silt content.

The effect of CTAB on silt settling process was simulated by the first-order kinetic mode (Eq. (1)) and the second-order kinetic mode (Eq. (2)) respectively. The results of correlation analysis were listed in Table 2. It can be indicated that the silt settlement in the presence of CTAB is more in line with the second-order kinetic mode.

$$\frac{1}{C_t} = kt + \frac{1}{C_0} \tag{1}$$

$$\ln C_t = -kt + \ln C_0 \tag{2}$$

where  $C_0$  and  $C_t$  represent the silt concentration of the section at 0 and  $t$ , and  $k$  is the attenuation coefficient.

#### 3.2. Settling velocity of silt in still water in the presence of ionic surfactants

The representative settling velocity in still water refers to the uniform settling rate when the suspended sediment concentration reaches 50% of the initial sediment concentration. The scatter plots of settling velocity with different ionic surfactant concentration were displayed in Fig. 3, which were fitted and analyzed under different kinds of ionic surfactant respectively. Results revealed that the exponential function fitting is more suitable for describing the variation pattern between the silt settling velocity and CTAB concentration. That is to say, the representative settling velocity increased exponentially with the increase of CTAB concentration. However, the linear function seems to be more suitable to describe the variation pattern between the silt settling velocity and LAS concentration. In other words, the silt settling velocity decreased linearly as the increase of LAS concentration.

As can be seen from Fig. 3, when CTAB concentration was 5, 10, 15 and 20 mg L<sup>-1</sup>, the silt settling rate in still water increased by 1.70%, 4.76%, 10.25% and 20.16% respectively, while the sedimentation rate decreased by 1.99%, 4.06%, 6.21%, and 8.46%, when

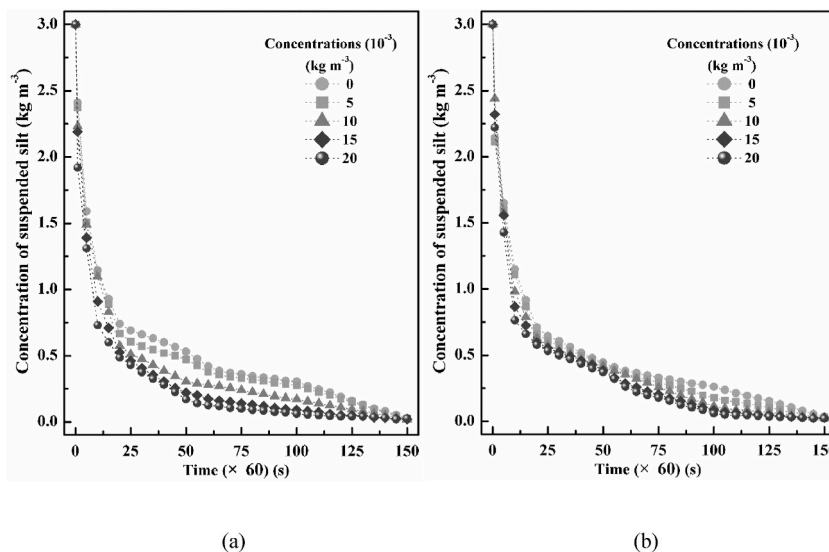


Fig. 2. Evolution of average suspended silt content (kg m<sup>-3</sup>) with different ionic surfactant concentrations. Left: (a) CTAB; Right: (b) LAS.

**Table 2**

The fitting results of the first-order and second-order kinetic equations influenced by CTAB.

Correlation coefficient	CTAB concentration ( $10^{-3}$ ) ( $\text{kg m}^{-3}$ )				
	0	5	10	15	20
First-order kinetic	0.936	0.932	0.957	0.969	0.940
Second-order kinetic	0.982	0.973	0.990	0.977	0.981

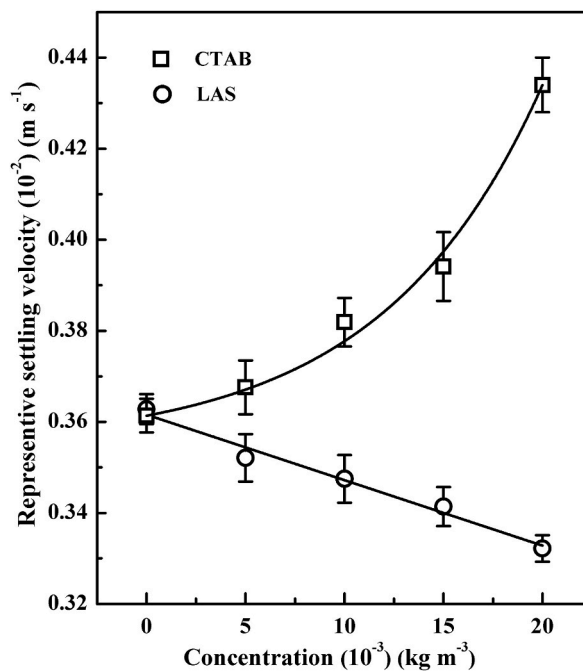


Fig. 3. Comparison of the representative settling velocity ( $\text{m s}^{-1}$ ) with the ionic surfactant concentration ( $\text{kg m}^{-3}$ ).

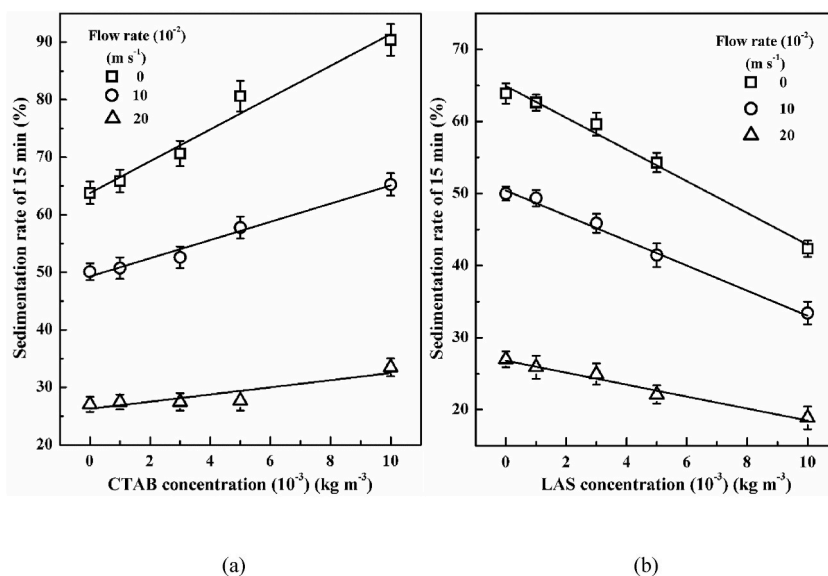


Fig. 4. Sedimentation rate of 15 min under different ionic surfactant concentration in flowing water. Left: (a) CTAB; Right: (b) LAS.

the LAS concentration was 5, 10, 15 and 20 mg L<sup>-1</sup>, respectively.

### 3.3. Settling velocity of silt in flowing water in the presence of ionic surfactants

Variations of particles settling velocity under different ionic surfactant concentration in flowing water were shown in Fig. 4. The settlement rate at 15 min was taken as the typical settling velocity. It was observed that the settling velocity increased with the increase of CTAB concentration while decreased with the increase of LAS concentration. The settling velocity was proportional to ionic surfactant concentration under the same flow rate, but the change trend was opposite for CTAB and LAS.

As shown in Fig. 4(a), the slopes of the linear line were different under different flow conditions. When the flow rate was 0, 10, 20 cm s<sup>-1</sup>, the slope was 2.773, 1.580, 0.628 respectively. That is to say, the influence of CTAB on sediment settlement decreases with the acceleration of flow rate. As seen in Fig. 4(b), when the flow velocity was 0, 10, 20 cm s<sup>-1</sup>, the slope was -2.196, -1.758, -0.827 respectively. It can be suggested that the impact of LAS on sediment settlement is weakened under the rapid flow. When the flow rate was 0, 10, 20 cm s<sup>-1</sup>, as the ionic surfactant concentration increased from 0 to 10 mg L<sup>-1</sup>, the corresponding settling velocity increased by 41.6%, 30.3% and 23.6% under the CTAB, but the corresponding settling velocity decreased by 33.6%, 33.2%, and 29.9% under LAS. In general, when the flow rate was 20 cm s<sup>-1</sup>, the sedimentation rates under the influence of CTAB and LAS decreased to 57% and 89% of those in still water, respectively.

### 3.4. SEM image test

SEM images of silt particles after 500 times magnification with or without ionic surfactants were shown in Fig. 5. All samples were tested after lyophilization. Under DI water conditions, both the size of particles and the gap between them were not uniform. With the addition of LAS under the concentration of 100 mg L<sup>-1</sup>, the silt particles were finer than those undisturbed sediment, which also indicated that the role of LAS can improve the dispersion of silt particles. When the same concentration of CTAB was added, the silt particles changed greatly. It can be seen that part of the silt particles aggregated into large flocs, resulting in great changes in surface physicochemical properties such as silt porosity and particle size, and eventually led to a significant increase in the settling velocity.

Ten typical particles were selected from each figure (Fig. 5(a–c)) for particle size calculation, and the average equivalent diameters of sediment particles were 70.5 μm, 58.4 μm and 103.75 μm under the influence of DI water, LAS and CTAB, respectively. The effect of ionic surfactant on sediment flocculation was further confirmed by the change of flocculation size.

The typical particle size of flocs  $D_f$  under different concentration of CTAB was obtained by SEM images. The magnification factor  $M$  of sediment particle size can be used to characterize the degree of sediment flocculation,  $M = D_f/d$ , and  $d$  is the typical particle size of the primary sediment particles. The degree of sediment flocculation under the influence of CTAB was shown in Table 3. It was shown that the degree of flocculation increases with the increase of CTAB concentration, and the flocculation degree  $M$  reached about 1.5 when the CTAB concentration increased to 100 mg L<sup>-1</sup>.

It is well known that the particle size of flocs is the most important factor affecting the settling velocity. The settling velocity of flocs  $\omega_f$  can be calculated from the following model (Eq. (3)) which proposed by Winterwerp [17,18] for monosized particles and with constant fractal dimension  $F$ . In addition, the settling velocity  $\omega_0$  of single particle sediment can be estimated from the simplified formula (Eq. (4)). The comparison between the measured values of settling velocity and the results of the above two calculation models was shown in Fig. 6. It can be indicated that the measured values of settling velocity are between the calculated value of the two models, and the flocculation not only changes the size of sediment but also varies the law of settling velocity.

$$\omega_f = \frac{10^{-8}}{18} \frac{\alpha}{\beta} g \frac{\rho_s - \rho_w}{\mu} d^{3-F} \frac{D_f^{F-1}}{1 + 0.15Re^{0.687}} \tag{3}$$

$$\omega_0 = \frac{10^{-4}}{25.6} \frac{\rho_s - \rho_w}{\rho_w} g \frac{d^2}{\nu} \tag{4}$$

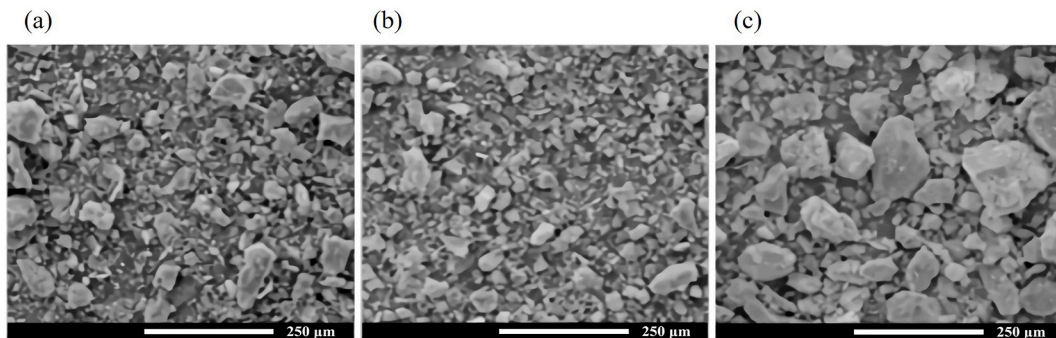


Fig. 5. SEM photographs (500 times magnification) of silt: (a) silt in the initial state; (b) silt after adsorption of the LAS; (c) silt after adsorption of the CTAB.

**Table 3**  
The degree of sediment flocculation under the influence of CTAB.

Concentration ( $10^{-3}$ ) ( $\text{kg m}^{-3}$ )	0	5	10	15	20
$D_f$ ( $10^{-6}$ ) (m)	70.5	72.4	74.3	76.1	79.6
$M$	1.000	1.027	1.054	1.079	1.129

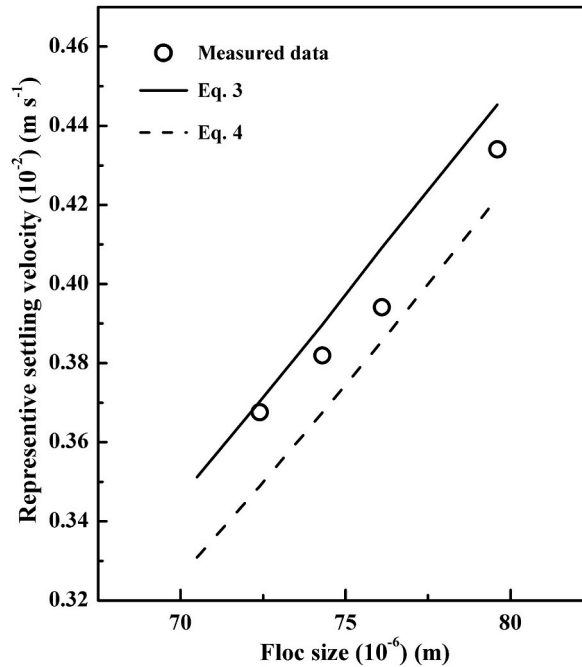


Fig. 6. Comparison between the measured values of settling velocity and the calculated results of the two models mentioned in this study.

where  $\alpha$  and  $\beta$  are shape-related coefficients and  $\alpha/\beta = 1$  for spherical particles,  $F$  is the three-dimensional fractal dimension of flocs,  $Re$  is the particle Reynolds number,  $\rho_s$  and  $\rho_w$  are the density of primary sediment particles and water,  $\mu$  and  $\nu$  are the dynamic viscosity and kinematic viscosity of water.

### 3.5. Zeta potential and surface tension of test

Zeta potential reflects a measure of the strength of mutual repulsion or attraction between particles. The smaller the molecular or dispersed particle size, the higher the absolute value of Zeta potential and the more stable the system, namely, dissolution or dispersion can resist aggregation. Conversely, the lower the absolute value of Zeta potential, the more prone to coagulation or agglomeration. As shown in Fig. 7, with the increase of CTAB concentration, the absolute value of Zeta potential decreased, and then the particles in solution tended to agglomerate, eventually led to an increase in settlement rate. Inversely, when the concentration of LAS increased, the absolute value of the Zeta potential increased and the settlement rate decreased. The surface tension evolution trend of test results (see Fig. 8) was similar to that shown in Fig. 7.

Results of Zeta potential and surface tension were consistent with the DLVO theory. The double electrical layer structure on the surface of sediment particles plays a leading role in the flocculation process. The electric double layer contains the adsorption layer (close to the particle surface) and the diffusion layer, as shown in Fig. 9. When the fine-grained silt is dispersed in a natural water, each particle is subjected to the dual action of van der Waals force and electrostatic repulsion. The particle reaches a stable state until the above two forces are balanced. However, once the ionic surfactant is added, the electric double layer on the particle surface changes, upsetting the previous equilibrium.  $\text{CTA}^+$  ions produced by the ionizing hydrolysis of CTAB compress the electric double layer, reducing the overlapping volume of the diffusion layer. As a result, the repulsive force between particles decreases, then the absolute value of the Zeta potential decreases and the surface tension increases. Finally, the flocculation is enhanced and the sedimentation rate is increased. However, LAS does exactly the opposite.



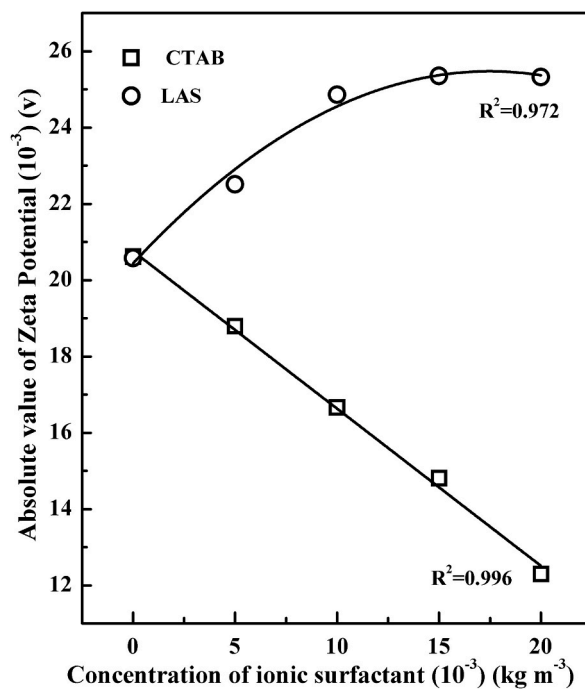


Fig. 7. The correlation between ionic surfactant concentrations and the Zeta potential of the water-silt system under the same initial silt concentration.

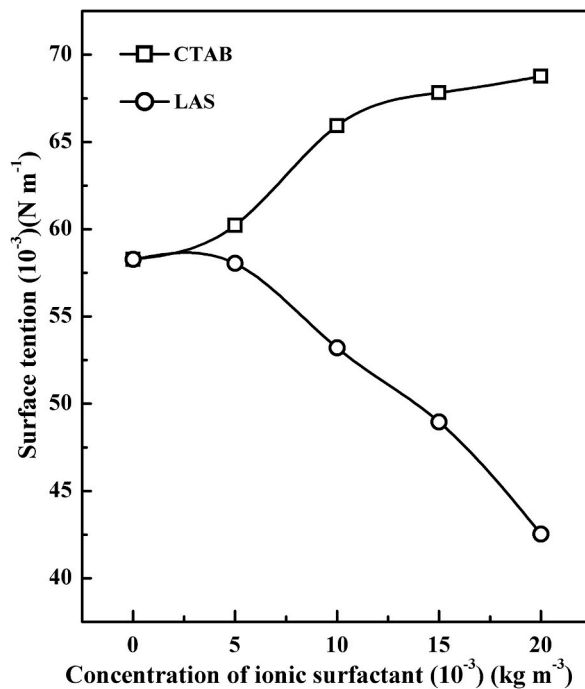


Fig. 8. The correlation between ionic surfactant concentrations and the surface tension of the water-silt system under the same initial silt concentration.



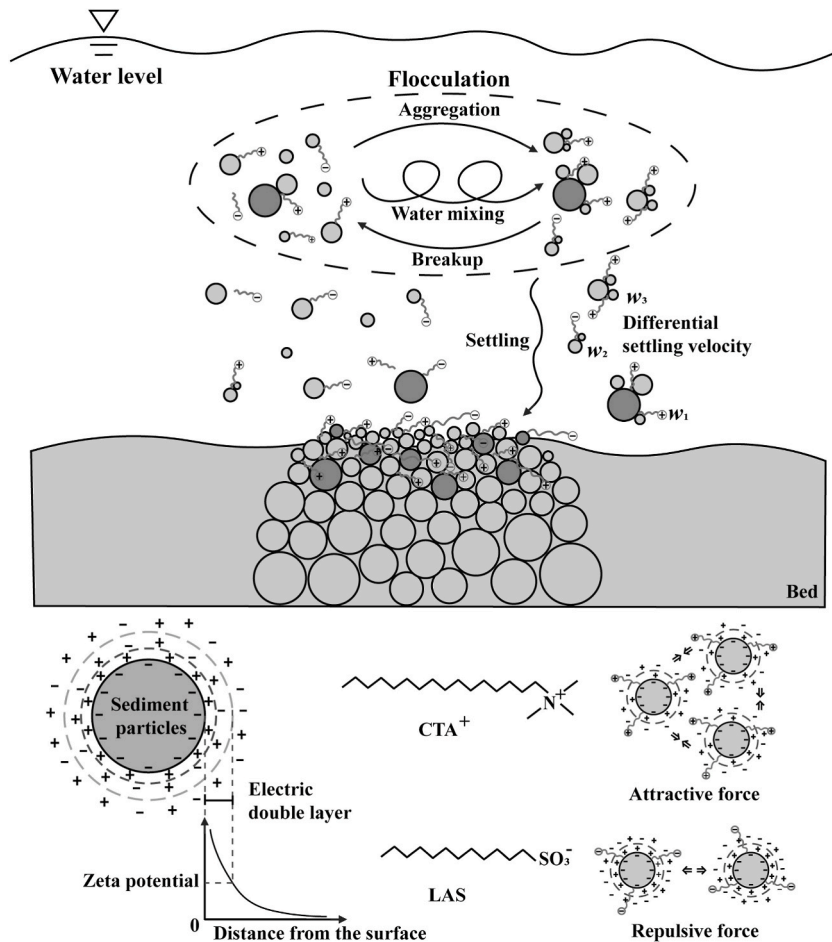


Fig. 9. The conceptual model of sediment-flocculation under the influence of ionic surfactants.

## 4. Discussion

### 4.1. Effects on the settling velocity of silt in still water

In still water, the settling velocity was found to have an exponential relationship with CTAB concentration, which is the same as the effect of suspended sediment concentration at low levels [19,20]. Similar to other cations such as  $\text{Na}^+$ ,  $\text{Ca}^{2+}$ ,  $\text{Mg}^{2+}$  and  $\text{Al}^{3+}$ , CTAB also affects the sediment settling velocity and Zeta potential because of the flocculation [21]. With the increase of cations concentration, the settling velocity increases and the absolute Zeta potential of sediment particles decreases. However, effects of different cations were different [5], which is consistent with the conclusion of this study. Conversely, LAS, as an anionic surfactant, repels the negative charge on the surface of silt particles, so it has little and negative influence on the flocculation and settling velocity. In general, the flocculation and sedimentation rate are mainly affected by the particles' irregular Brownian motion and the concentration of different kinds of ionic surfactant in still water.

### 4.2. Effects on the settling velocity of silt in flowing water

In flowing water, the effect law of ionic surfactants on silt settlement is the same as that in still water. However, the promotion effect of ionic surfactant on the floc size sedimentation rate was weakened with the increase of flow rate. The largest settling velocity occurred in still water because turbulence plays an inhibitory role in the flocculation process, which is consistent with previous studies. Brownian motion is no longer the main factor affecting sediment flocculation in flowing water due to the change of the sediment surface charge under the electrochemical reaction with ions in electrolyte. With the increase of velocity, strong collisions caused by turbulence and shear become dominant. If the collision is large enough for the kinetic energy of particles to overcome the bonding force between them, the flocs will break up or disintegrate. Therefore, under high flow rate conditions, turbulence and shear will retard flocculation and reduce the settlement of silt. In addition, different kinds of ionic surfactants have different responses to the change of flowing water condition. The weakening influence of CTAB is more significant than that of LAS. This is because the flocculation is weak

under the condition of LAS concentration, and there are fewer flocs, especially large flocs, in flowing water. The main effect of turbulence and shear is to promote particle diffusion, so the sedimentation rate of particles is less affected. In addition, the critical values of turbulent shearing rate which exist in the formation process of flocs [22–24] were not captured in this experiment.

## 5. Conclusion

The potential effects of two kinds of typical ionic surfactants on the settling velocity of natural fine-grained cohesive sediment and its internal influencing mechanism were investigated. Ionic surfactants, especially cationic surfactants, have significant effects on the flocculation process of silt particles. The size and surface characteristics (such as Zeta potential, surface tension) of flocs vary with the types and concentrations of ionic surfactant, resulting in the changes in sedimentation rate and sedimentation law. In addition, under the turbulent condition, the effect of ionic surfactants on silt settlement is weakened because of the enhanced dispersion of silt particles and the broken up of flocs. Especially at high flow rates, turbulence plays a leading role in the flocculation process.

This research will benefit to understand the flocculation and sedimentation of fine-grained cohesive sediment in natural water under the action of ionic surfactants, and the method can also be used to studying the flocculation mechanism under the joint action of multiple factors, such as the composite influencing factors of electrochemistry and organic matter. Furthermore, the results of this study are expected to be used for particle size distribution of fine-grained soil based on the difference of sedimentation rate under the action of ionic surfactants.

## Funding

This work is supported by a grant from the National Key Research and Development Program of China [Project Number: 2022YFE0117000].

## Author contribution statement

Zhuo Huang: Conceived and designed the experiments; (2) Analyzed and interpreted the data; (3) Wrote the paper.

Yuan Xiang: Analyzed and interpreted the data; (2) Wrote the paper.

Yue-Xiao Liu: Performed the experiments; (2) Contributed reagents, materials, analysis tools and data; (3) Wrote the paper.

Guang-Fang Li: Contributed reagents, materials, and data; (2) Wrote the paper.

Hui-Qun Cao: Contributed reagents, materials and data analysis; (2) Wrote the paper.

## Data availability statement

Data will be made available on request.

## Additional information

Supplementary content related to this article has been published online at [URL].

## Declaration of competing interest

The authors declare that they have no known competing financial interests or personal relationships that could have appeared to influence the work reported in this paper.

## Acknowledgement

The author wishes to thank all those who contributed to the paper and the anonymous reviewers. They have greatly improved the clarity of the text.

## Notation

$C_0$	silt concentration of the section at time 0 ( $\text{kg m}^{-3}$ )
$C_t$	silt concentration of the section at time $t$ ( $\text{kg m}^{-3}$ )
$k$	attenuation coefficient (–)
$D_f$	typical particle size of flocs (m)
$d$	typical particle size of the primary sediment particles (m)
$M$	magnification factor of sediment particle (–)
$F$	constant fractal dimension (–)
$Re$	particle Reynolds number (–)
$\omega_f$	settling velocity of flocs ( $\text{m s}^{-1}$ )
$\omega_0$	settling velocity of single particle sediment ( $\text{m s}^{-1}$ )

$\alpha, \beta$	shape-related coefficients (–)
$\rho_s$	density of primary sediment particles ( $\text{kg m}^{-3}$ )
$\rho_w$	water density ( $\text{kg m}^{-3}$ )
$\mu$	dynamic viscosity of water ( $\text{N s m}^{-2}$ )
$\nu$	kinematic viscosity of water ( $\text{m}^2 \text{s}^{-1}$ )

## References

- [1] G. Ying, Fate, behavior and effects of surfactants and their degradation products in the environment, *Environ. Int.* 32 (3) (2006) 417–431, <https://doi.org/10.1016/j.envint.2005.07.004>.
- [2] M.J. Scott, M.N. Jones, The biodegradation of surfactants in the environment, *Biochim. Biophys. Acta Biomembr.* 1508 (1–2) (2000) 235–251, [https://doi.org/10.1016/S0304-4157\(00\)00013-7](https://doi.org/10.1016/S0304-4157(00)00013-7).
- [3] D. Liang, X. Wang, B.N. Bockelmann-Evans, R.A. Falconer, Study on nutrient distribution and interaction with sediments in a macro-tidal estuary, *Adv. Water Resour.* 52 (FEB.) (2013) 207–220, <https://doi.org/10.1016/j.advwatres.2012.11.015>.
- [4] Y. Wang, G. Voulgaris, Y. Li, Y. Yang, J. Gao, J. Chen, S. Gao, Sediment resuspension, flocculation, and settling in a macrotidal estuary, *Journal of Geophysical Research Oceans* 118 (10) (2013) 5591–5608, <https://doi.org/10.1002/jgrc.20340>.
- [5] F. Mietta, C. Chassagne, A.J. Manning, J.C. Winterwerp, Influence of shear rate, organic matter content, pH and salinity on mud flocculation, *Ocean Dynam.* 59 (5) (2009) 751–763, <http://link.springer.com/article/10.1007/s10236-010-0330-2>.
- [6] C. Guo, Q. He, L. Guo, J.C. Winterwerp, A study of in-situ sediment flocculation in the turbidity maxima of the Yangtze Estuary, *Estuar. Coast Shelf Sci.* 191 (MAY15) (2017) 1–9, <https://doi.org/10.1016/j.ecss.2017.04.001>.
- [7] J.F. Zhang, Q.H. Zhang, P.Y. Maa, G. Qiao, Lattice Boltzmann simulation of turbulence-induced flocculation of cohesive sediment, *Ocean Dynam.* 63 (9–10) (2013) 1123–1135, <https://link.springer.com/article/10.1007/s10236-013-0646-9>.
- [8] X.L. Tan, G.P. Zhang, H. Yin, A.H. Reed, Y. Furukawa, Characterization of particle size and settling velocity of cohesive sediments affected by a neutral exopolymer, *Int. J. Sediment Res.* 27 (4) (2012) 473–485, [https://doi.org/10.1016/S1001-6279\(13\)60006-2](https://doi.org/10.1016/S1001-6279(13)60006-2).
- [9] Y. Furukawa, A.H. Reed, G.P. Zhang, Effect of organic matter on estuarine flocculation: a laboratory study using montmorillonite, humic acid, xanthan gum, guar gum and natural estuarine flocs, *Geochem. Trans.* 15 (1) (2014) 1, <https://geochemicaltransactions.biomedcentral.com/articles/10.1186/1467-4866-15-1>.
- [10] X. Shen, E.A. Toorman, B.J. Lee, M. Fettweis, Biophysical flocculation of suspended particulate matters in Belgian coastal zones, *J. Hydrol.* 567 (2018) 238–252, <https://doi.org/10.1016/j.jhydrol.2018.10.028>.
- [11] X.M. Xia, Y. Li, H. Yang, C.Y. Wu, T.H. Sing, H.K. Pong, Observations on the size and settling velocity distributions of suspended sediment in the Pearl River Estuary, China, *Contin. Shelf Res.* 24 (16) (2004) 1809–1826, <https://doi.org/10.1016/j.csr.2004.06.009>.
- [12] Y.L. Lau, Temperature effect on settling velocity and deposition of cohesive sediments, *J. Hydraul. Res.* 32 (1) (1994) 41–51, <https://doi.org/10.1080/00221689409498788>.
- [13] S.B. Ummalyma, A.K. Mathew, A. Pandey, R.K. Sukumaran, Harvesting of microalgal biomass: efficient method for flocculation through pH modulation, *Bioresour. Technol.* 213 (2016) 216–221, <https://doi.org/10.1016/j.biortech.2016.03.114>.
- [14] Y. Wan, H. Wu, D. Roelvink, F. Gu, Experimental study on fall velocity of fine sediment in the Yangtze Estuary, China, *Ocean Eng.* 103 (2015) 180–187, <https://doi.org/10.1016/j.oceaneng.2015.04.076>.
- [15] L.I. Portela, S. Ramos, A.T. Teixeira, Effect of salinity on the settling velocity of fine sediments of a harbour basin, *J. Coast Res.* 165 (Part 2, Sp. Iss. 65) (2016) 1188–1193, <https://doi.org/10.2112/SI65-201.1>.
- [16] M. Kim, S. Kim, J. Kim, S. Kang, S. Lee, Factors affecting flocculation performance of synthetic polymer for turbidity control, *J. Agric. Chem. Environ.* 2 (1) (2013) 16–21, <https://doi.org/10.4236/jacen.2013.21003>.
- [17] J.C. Winterwerp, A simple model for turbulence induced flocculation of cohesive sediment, *J. Hydraul. Res.* 36 (3) (1998) 309–326, <https://doi.org/10.1080/00221689809498621>.
- [18] A. Khelifa, P.S. Hill, Models for effective density and settling velocity of flocs, *J. Hydraul. Res.* 44 (3) (2006) 390–401, <https://doi.org/10.1080/00221686.2006.9521690>.
- [19] K.L. Priya, P. Jegathambal, E.J. James, On the factors affecting the settling velocity of fine suspended sediments in a shallow estuary, *J. Oceanogr.* 71 (2) (2015) 163–175, <https://link.springer.com/article/10.1007/s10872-014-0269-x>.
- [20] J.C. Winterwerp, A.J. Manning, C. Martens, T. Mulder, J. Vanlede, A heuristic formula for turbulence-induced flocculation of cohesive sediment, *Estuar. Coast Shelf Sci.* 68 (1–2) (2006) 195–207, <https://doi.org/10.1016/j.ecss.2006.02.003>.
- [21] Y. Ou, R. Li, R. Liang, Experimental study on the impact of NaCl concentration on the flocculating settling of fine sediment in static water, *Procedia Eng.* 154 (2016) 529–535, <https://doi.org/10.1016/j.proeng.2016.07.548>.
- [22] I. Safak, M.A. Allison, A. Sheremet, Flocc variability under changing turbulent stresses and sediment availability on a wave energetic muddy shelf, *Contin. Shelf Res.* 53 (2013) 1–10, <https://doi.org/10.1016/j.csr.2012.11.015>.
- [23] F. Maggi, F. Mietta, F. Winterwerp, Effect of variable fractal dimension on the floc size distribution of suspended cohesive sediment, *J. Hydrol.* 343 (1–2) (2007) 43–55, <https://doi.org/10.1016/j.jhydrol.2007.05.035>.
- [24] R.G. Kumar, K.B. Strom, A. Keyvani, Flocc properties and settling velocity of San Jacinto estuary mud under variable shear and salinity conditions, *Contin. Shelf Res.* 30 (20) (2010) 2067–2081, <https://doi.org/10.1016/j.csr.2010.10.006>.